



Received on 05 January 2020; received in revised form, 08 April 2020; accepted, 11 April 2020; published 01 January 2021

CYTOPROTECTIVE ROLE OF ENCAPSULATED ASTAXANTHIN AGAINST HEPATOCELLULAR CARCINOMA (HepG2) CELL LINE

V. Suganya and V. Anuradha *

PG and Research Department of Biochemistry, Mohamed Sathak College of Arts & Science, Sholinganallur, Chennai - 600119, Tamil Nadu, India.

Keywords:

Hepatocellular carcinoma (HCC), Sorafenib, Liposomal encapsulation, Astaxanthin, Flow cytometry

Correspondence to Author:

Dr. V. Anuradha

Assistant Professor,
PG and Research Department of
Biochemistry, Mohamed Sathak
College of Arts & Science,
Sholinganallur, Chennai - 600119,
Tamil Nadu, India.

E-mail: vanuradha2712@gmail.com

ABSTRACT: Astaxanthin (3,3'-dihydroxy- β , β' -carotene-4,4'-dione) is a xanthophyll carotenoid, which is found in *Haematococcus pluvialis*, *Chlorella zofingiensis*, *Chlorococcum*, and *Phaffiarhodozyma*. Astaxanthin play major role as a nutritional supplement, antioxidant and anticancer agent, anti-diabetes, cardiovascular diseases, and neurodegenerative disorders. In our previous study, astaxanthin was first encapsulated by different agents and characterized using SEM, FT-IR, and *in-vitro* drug release. The present study aimed to explore the anticancer activity of encapsulated and non-encapsulated astaxanthin on the African green monkey normal kidney Vero cell line and HepG2 cell line. From the *in-vitro* study, the IC₅₀ of HepG2 cells was found to be 500 μ g/ml compared to the normal Vero cell line with IC₅₀ of 600 μ g/ml of which was confirmed by MTT assay. Further, the fluorescence microscope and DNA fragmentation were carried to analyze the apoptosis in HepG2 treated cells. Thus, our results suggested that liposomal encapsulated astaxanthin (ME1) exhibits good anticancer activity when compared amongst other test samples and positive drug sorafenib.

INTRODUCTION: Cancer is progressively a serious health problem and one of the foremost causes of death in the world. Changes in lifestyle, aging, population, and the adoption of cancer-causing behavior are some of the reasons for this pervasiveness. According to cancer statistics in 2013, in Asia, stomach and liver cancer is the most common, and both are associated with high impermanence rates, though bladder cancer is the most common in the USA. Colorectal and breast cancers have high-frequency rates in all countries. Chemotherapy, radiotherapy, and chemically derived drugs are the current treatment in India.

Chemotherapy treatment makes the patient under a lot of strain and also causes damage to their health. Therefore, there is a focus on using alternative treatments using some natural drugs against cancer disease¹.

Hepatocellular carcinoma (HCC) is the sixth most common malignancy and the third most regular cause of cancer death. HCC presents with high-frequency rates of 80% in the developing countries in East Asia and sub-Saharan Africa. Furthermore, maximum HCC patients have deprived prognosis and show resistance to chemotherapy². Surgery, local treatment, and liver transplantation may provide a therapeutic perspective for patients with HCC; only 10-20% of patients are eligible for therapeutic treatments³. Furthermore, traditional systemic chemotherapy does not provide survival benefits in patients with HCC. Molecular targeted therapy shows promise for HCC treatment.

<p>QUICK RESPONSE CODE</p> 	<p>DOI: 10.13040/IJPSR.0975-8232.12(1).372-84</p> <hr/> <p>This article can be accessed online on www.ijpsr.com</p> <hr/> <p>DOI link: http://dx.doi.org/10.13040/IJPSR.0975-8232.12(1).372-84</p>
---	---

Carcinogenesis usually arises as a consequence of chemical or biological damage to normal cells in a multistep and multifactor process composed of genetic derangement, aberrant signal transduction, and protein kinase activation. These processes consist of three stages in cancer development, such as initiation, promotion, and progression. Among these three stages, the promotion stage is reversible and appears to be the maximum target stage for chemopreventive intervention⁴.

Sorafenib (Nexavar) is the first and only molecular targeted therapy approved by the U.S. Food and Drug Administration in 2007 for the treatment of HCC. Sorafenib displays a remarkable inhibition of Raf-1 and other tyrosine kinases, which is a multiple kinase inhibitor that includes vascular endothelial growth factor receptor 2 (VEGFR2), VEGFR3, Flt-3, platelet-derived growth factor (PDGF), and fibroblast growth factor receptor-1 (FGFR-1)⁵. While sorafenib showed survival benefits in enormous randomized phase III studies, the reaction rate is relatively low^{6,7}.

Astaxanthin (3,3'-dihydroxy- β,β' -carotene-4,4'-dione) is a xanthophyll carotenoid⁸ which naturally occurs in algae, krill, trout, crayfish, and salmon. Astaxanthin is widely used in aquaculture nutrition as a coloring agent⁹. Astaxanthin has two chiral centers at positions 3 and 3'. The astaxanthin stereoisomer -3*S*,3*S'*- is the main form found in wild salmon¹⁰. Most astaxanthin used in aquaculture nutrition is produced synthetically, which yields three different stereoisomers, including 3*S*, 3'*S*; 3*R*, 3'*S*; and 3*R*, 3'*R*. It has shown strong biological activities, including antioxidant effects, anti-lipid peroxidation activity, anti-inflammation, cardiovascular disease prevention, and immune-modulation effects compared with other carotenoids⁸. Previous evidence suggests that astaxanthin has anti-cancer efficacy in multiple types of cancer. *In-vivo* anticancer activity of astaxanthin in hepatocellular carcinoma was reported^{11, 12}. The anti-cancer effects of astaxanthin are reportedly attributed to its effects on the pathological process of cancer cells through a variety of pathways, including apoptosis, inflammation, and cell junction.

In this article, we have presented the anti-proliferative potential of encapsulated and non-

encapsulated astaxanthin in HCC tumors in HepG2 cell lines through MTT assay, DNA fragmentation, Assessment of apoptosis, and flow cytometry.

MATERIALS AND METHODS:

Sample Preparation:

A. Non-encapsulated Astaxanthin: Free pure form of Astaxanthin (red color) powder was purchased from Rudra Bio ventures Pvt., Ltd, Bangalore.

B. Microencapsulated Astaxanthin:¹³ Sodium alginate encapsulated astaxanthin (ME1)^{14, 15}, Alginate-chitosan encapsulated astaxanthin (ME2)¹⁶⁻¹⁸. Chitosan-TPP encapsulated astaxanthin (ME3)^{19, 20}. Liposome encapsulated astaxanthin (ME4)²¹.

C. Positive Drug: Sorafenib a positive drug, was purchased from Sigma-Aldrich, India.

Cell Culture Maintenance: Vero African green monkey kidney normal cell line, HepG2 hepatocellular carcinoma cancer cell line was obtained from the National Centre for Cell Sciences (NCCS), Pune, India. In DMEM medium, cells were maintained in the logarithmic phase of growth, which is supplemented with 10% (v/v) heat-inactivated fetal bovine serum, 100 U/ml penicillin, 100 μ g/ml streptomycin. They were maintained at 37 °C with 5% CO₂ - 95% air humidified incubator.

Effect of Microencapsulated and non-Encapsulated Astaxanthin on Cytotoxicity of Cell Lines - MTT Assay:

The cytotoxic effect of microencapsulated and non-encapsulated astaxanthin along with positive drug sorafenib was tested against both normal cell line Vero and cancer cell lines of HepG2 by MTT (3-(4,5-dimethylthiazol-2-yl)-2,5-diphenyltetrazolium bromide) assay²². Briefly, the cell lines were separately seeded in 96-well microplates (1 \times 10⁶ cells/ml) and incubated for 24 h at 37 °C with 5% CO₂ incubator and allowed them to grow to 90% convergence. At the end of the incubation, the medium was replaced and the Vero cells were treated with microencapsulated, non-encapsulated astaxanthin and sorafenib at different concentrations of 200, 400, 600, 800, and 1000 μ g/ml. Consequently, hepatic cancer cell line HepG2 was also treated with microencapsulated and non-encapsulated astaxanthin along with positive drug sorafenib at

same concentrations, which were incubated for 24 h. Formerly, for additional 4 h the cells were then washed with phosphate-buffered saline (PBS, pH-7.4) and added 20 μ l of (MTT) solution (5 mg/ml) to each well and allowed to stand at 37 °C in the dark. Finally, 100 μ l DMSO was added and dissolved in the formazan crystals, and the absorbance was read spectrophotometry at 570 nm using an ELISA plate reader. The percentage of cell viability was expressed as:

$$\text{Cell viability (\%)} = \frac{\text{Absorbance of treated cells} \times 100}{\text{Absorbance of control cells}}$$

Analysis of Morphological Changes: The concentration that inhibited 50% of cell growth was referred as IC₅₀ value, which was used as a parameter for cytotoxicity study. The morphological changes of untreated (control) and the cells treated at IC₅₀ were observed under a bright field microscope after 24 h and photographed.

Assessment of Apoptosis:

Propidium Iodide (PI) Nucleic Acid Stain: HepG2 cells were plated at 5×10^4 cells/well into a six-well chamber plate. At N90% confluence, the cells were treated with microencapsulated and non-encapsulated astaxanthin along with positive drug sorafenib for 24 h. The cells were washed with PBS fixed in methanol: acetic acid (3:1, v/v) for 10 min and stained with 50 μ g/ml Propidium iodide (PI) for 20 min. The nuclear morphology of apoptotic cells was examined under FLoId Cell Imaging fluorescent microscopy²³.

Acridine Orange (AO)/Ethidium Bromide (EB) Dual Staining: Cell death was determined by the method of²³. The HepG2 cells were seeded in 6-well plates and treated with IC₅₀ concentration of microencapsulated and non-encapsulated astaxanthin along with positive drug sorafenib for 24 h. For the nuclear analysis, the monolayer of cells was washed with PBS and stained with 5 μ l of acridine orange (100 μ g/ml) and 5 μ l of ethidium bromide (100 μ g/ml). The morphological changes in the stained cells, the apoptotic nuclei (intensely stained, fragmented nuclei, and condensed chromatin) were observed by FLoId Cell Imaging fluorescent microscopy.

Analysis of DNA Fragmentation: DNA extraction and Agarose Gel Electrophoresis were performed

by following standard method²⁴. Briefly, HepG2 cancer cells (1×10^6 cells/ml) were plated per well in 6well plates with DMEM medium containing 10% FBS. The cells were then incubated for 24 h under 5% CO₂ at 37 °C. Then the medium was removed, washed with PBS, fresh serum-free medium was added, and kept in a CO₂ incubator at 37 °C for 1 h. After starvation, the cells were treated with IC₅₀ concentration of micro-encapsulated and non-encapsulated astaxanthin along with positive drug sorafenib for 24 h. After incubation, the DNA was extracted from cell lysate as follows: The cells were washed with PBS followed by the addition of 0.5 ml of lysis buffer and transferred into a microfuge tube. This mixture was incubated for 1 h at 37 °C, and to this, 4 μ l of proteinase K was added, incubated at 50 °C for 3 h. To each sample, 0.5 ml of phenol: chloroform: isoamyl alcohol (25:24:1) was added, mixed, and centrifuged at 10,000 rpm for 10 min at 4 °C. After centrifugation, to the supernatant 2 volumes of absolute ice-cold ethanol and 1/10 volume of 3 M sodium acetate were added and incubated for 30 min on ice to precipitate DNA. DNA was pelleted by centrifugation at 13,000 rpm for 10 min at 4 °C.

The supernatant was aspirated, and the pellet was washed with 1.0 ml of 70% ethanol. The centrifugation process was repeated until the last traces were removed, and the pellet was allowed to dry at room temperature for approximately 30 min and resuspended in 50 μ l of TE buffer. 10 μ g/ml of DNA samples were electrophoresed in 1% agarose gel contained ethidium bromide in a gel tank containing TBE buffer for 1 h under 90 V. The gels were examined under a UV transilluminator, Biorad.

Analysis of Cell Cycle: The cell cycle phase's distribution and measurement were recorded by following the standard method²⁵. Briefly, after treatment, floating cells in the medium were pooled with attached cells collected by trypsinization. Cells were washed with ice-cold PBS and fixed in 80% ethanol in PBS at -20 °C. The fixed cells were pelleted and stained with PI (50 μ g/ml) in the presence of RNase A (20 μ g/ml) for 30 min at 37 °C. About $\geq 20,000$ cells were analyzed in a Becton Dickinson FAC scan flow cytometer. Cell cycle histograms were analyzed using Cell Quest software.

Statistical Analysis: All the data were evaluated using PASW statistics 18 software. The hypothesis testing method included a One-way analysis of variance (ANOVA) followed by a significant difference test. $p < 0.05$ was considered to indicate statistical significance. All the results were expressed as mean \pm standard deviation (SD) for each test.

RESULTS: Astaxanthin and Sorafenib play a key role in industrial, pharmaceutical, and biomedical applications. Cellular elucidation to the antioxidants molecules may be subject to changes in cell morphology, the rate of cell growth or cell death. We examined cell viability through the test drug non-encapsulated and encapsulated astaxanthin along with positive drug sorafenib by MTT assay. The strategic parameters in evaluating the

biocompatibility of test drug are cytotoxicity and cell viability. The cytotoxicity of test drugs against vero cells was examined by MTT assay.

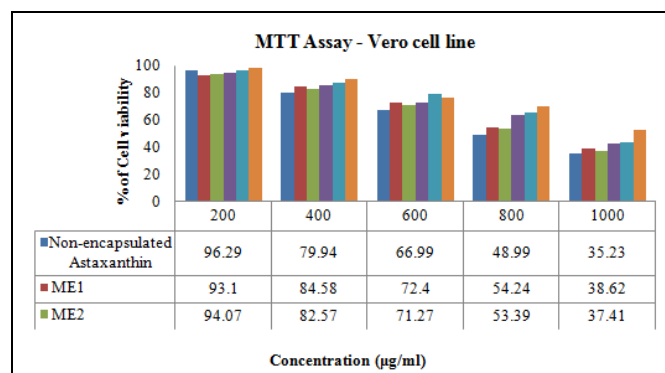


FIG. 1: CYTOTOXICITY OF NON-ENCAPSULATED AND ENCAPSULATED ASTAXANTHIN ALONG WITH SORAFENIB AGAINST VERO (NORMAL) CELL LINE. NS- Not Significant, ** ($p > 0.01$), * ($p > 0.05$), $n = 10$ values are mean \pm S.D (One way ANOVA followed by Dunnett's test).

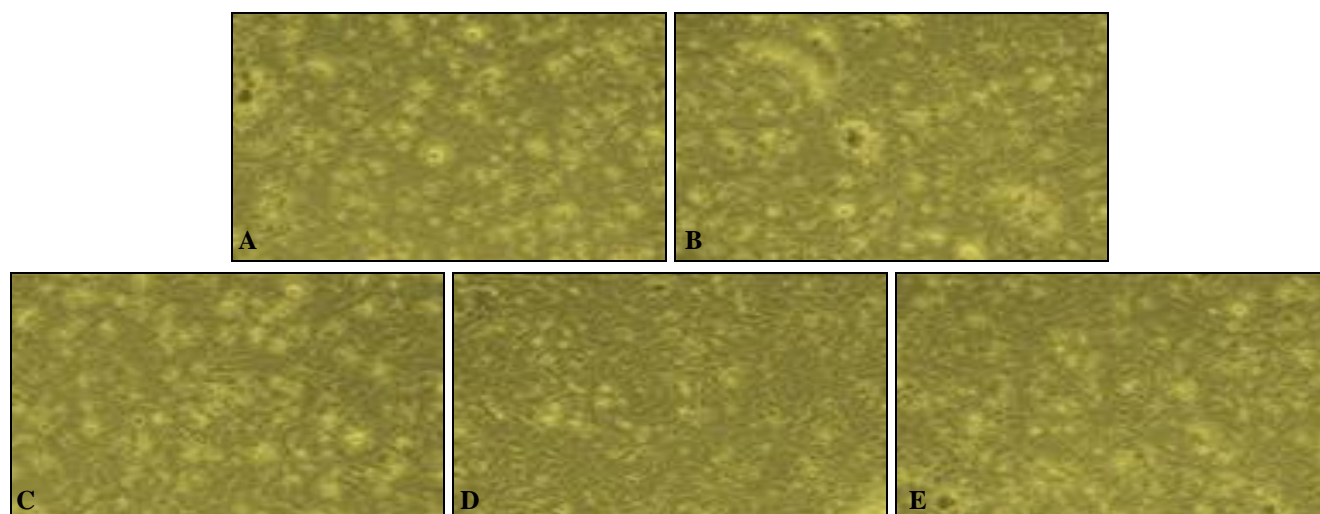


FIG. 2: MORPHOLOGICAL ANALYSIS OF NON-ENCAPSULATED ASTAXANTHIN AGAINST VERO CELL LINE – MTT ASSAY

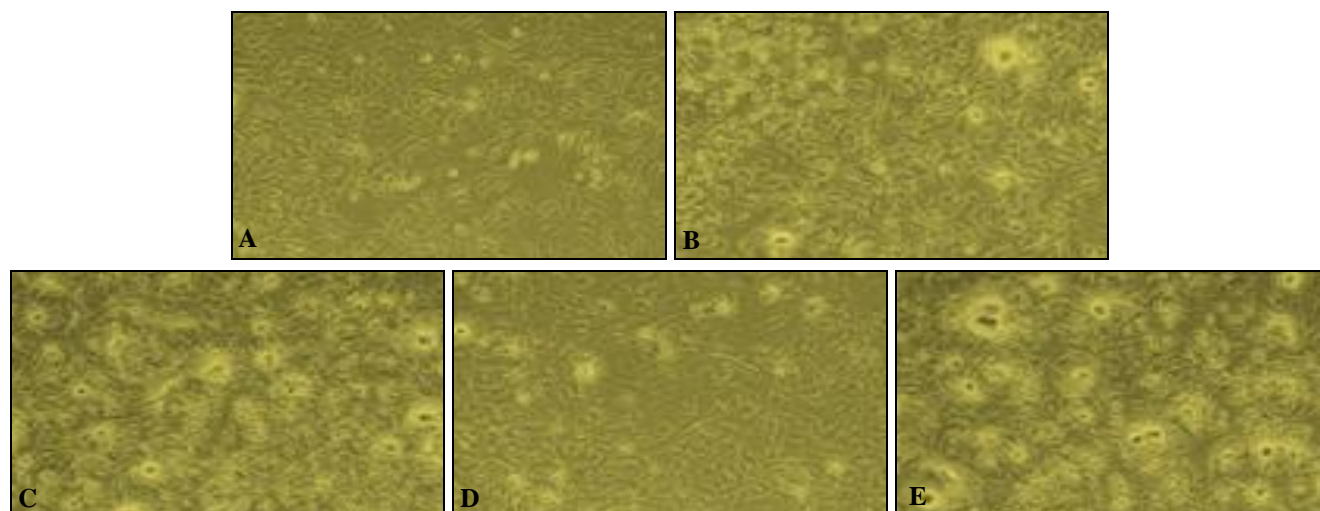


FIG. 3: MORPHOLOGICAL ANALYSIS OF ENCAPSULATED ASTAXANTHIN (ME1) AGAINST VERO CELL LINE – MTT ASSAY

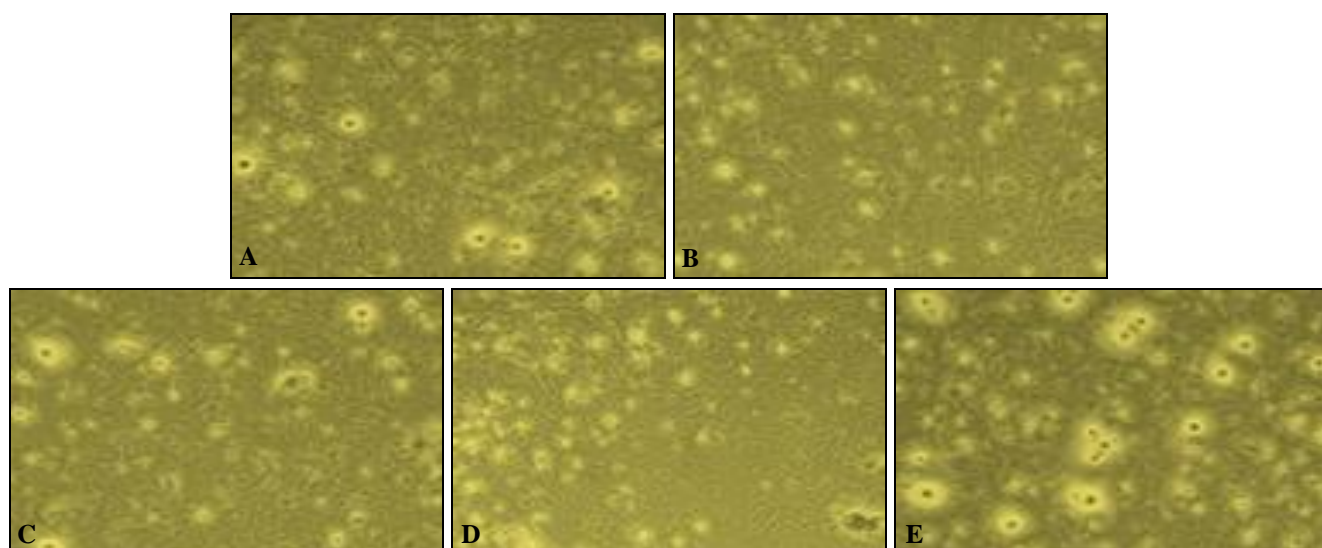


FIG. 4: MORPHOLOGICAL ANALYSIS OF ENCAPSULATED ASTAXANTHIN (ME2) AGAINST VERO CELL LINE – MTT ASSAY

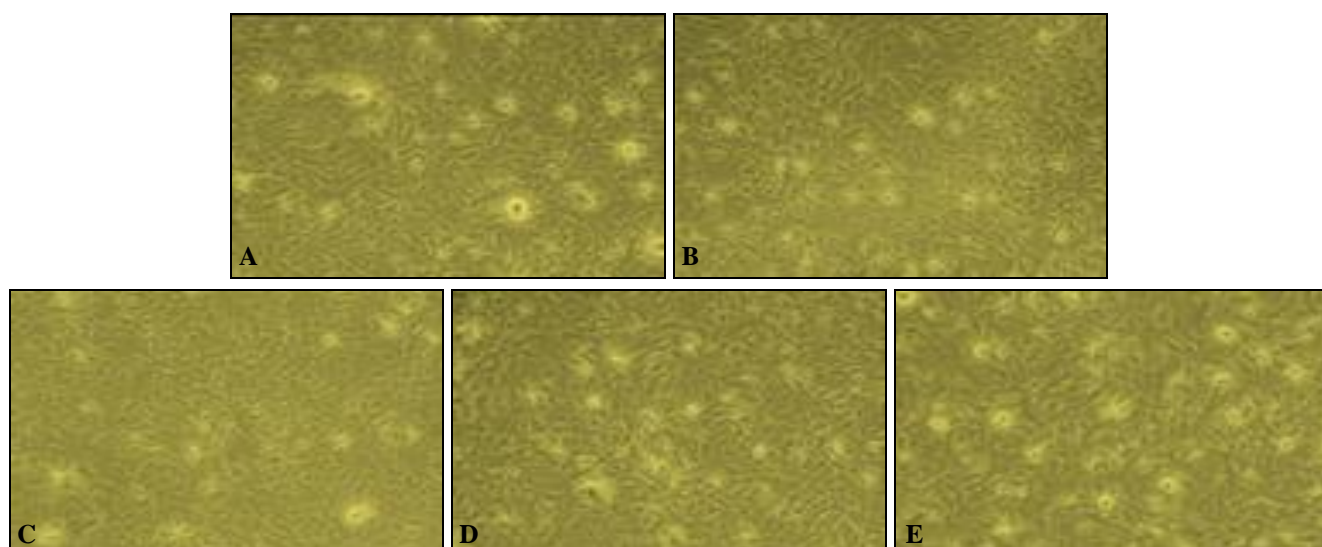


FIG. 5: MORPHOLOGICAL ANALYSIS OF ENCAPSULATED ASTAXANTHIN (ME3) AGAINST VERO CELL LINE – MTT ASSAY

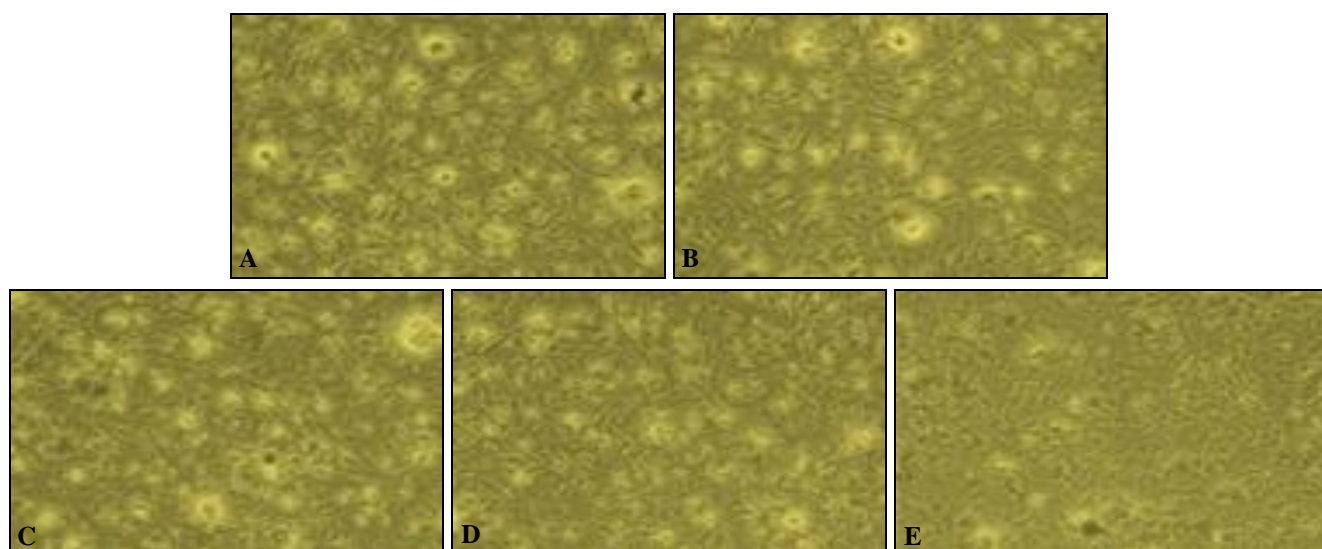


FIG. 6: MORPHOLOGICAL ANALYSIS OF ENCAPSULATED ASTAXANTHIN (ME4) AGAINST VERO CELL LINE – MTT ASSAY

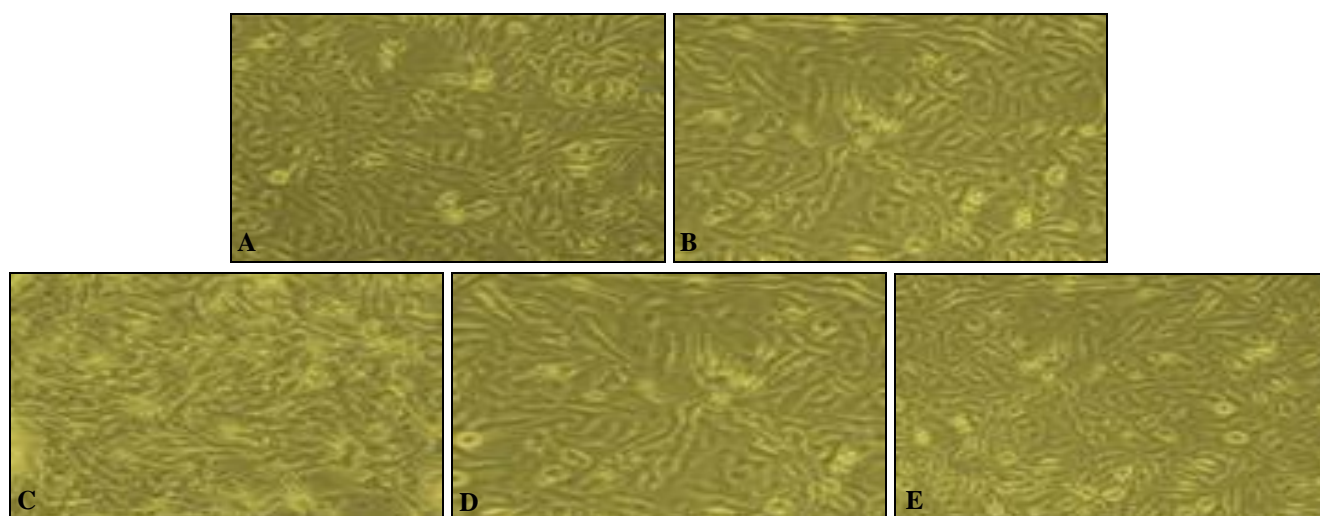


FIG. 7: MORPHOLOGICAL ANALYSIS OF POSITIVE DRUG SORAFENIB AGAINST VERO CELL LINE – MTT ASSAY. Note: A- 200 µg/ml; B – 400 µg/ml; C – 600 µg/ml; D – 800 µg/ml; E – 1000 µg/ml

The effect of non-encapsulated and encapsulated astaxanthin along with positive drug sorafenib at different concentrations such as 200, 400, 600, 800 and 1000 µg/ml on cell viability of vero (Normal) cells was made at 24 h, 48 h, 72 h, and 96 h respectively. The cells showed 80-85% viability up to the concentration 800 µg/ml. Moreover, above 90-95% indicates the adaptation of vero cells in all studies concentrations due to increased biocompatibility and increased incubation time. The cytotoxicity effects of test drugs on vero cells were examined using MTT assay and represented in **Fig. 1- 7**. The overall IC_{50} value of 600 µg/ml was obtained by all the studied drugs ($p < 0.05$). ME4 encapsulated astaxanthin showed better biocompatibility when compared to other types of encapsulated astaxanthin and free astaxanthin. Significantly we founded that there are decreases in cell viability of astaxanthin (encapsulated and non-encapsulated) treated groups when compared to

sorafenib treated group **Fig. 1**. The cell viability assay made in the present investigation indicated that liposomal encapsulated astaxanthin ME4 and sorafenib are less toxic when compared with rest of the test drugs.

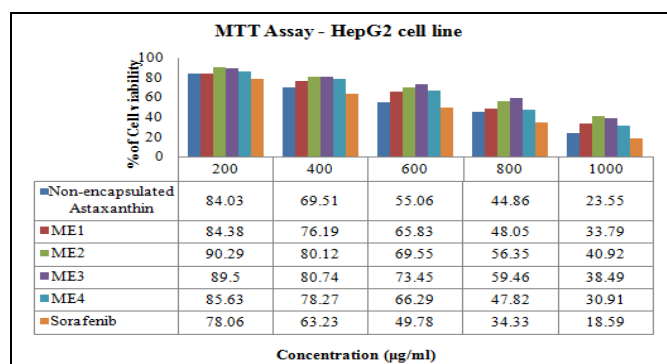


FIG. 8: CYTOTOXICITY OF NON-ENCAPSULATED AND ENCAPSULATED ASTAXANTHIN ALONG WITH SORAFENIB AGAINST HepG2 (LIVER CANCER) CELL LINE. NS- Not Significant, ** ($p > 0.01$), * ($p > 0.05$), $n = 10$ values are mean \pm S.D (One way ANOVA followed by Dunnett's test).

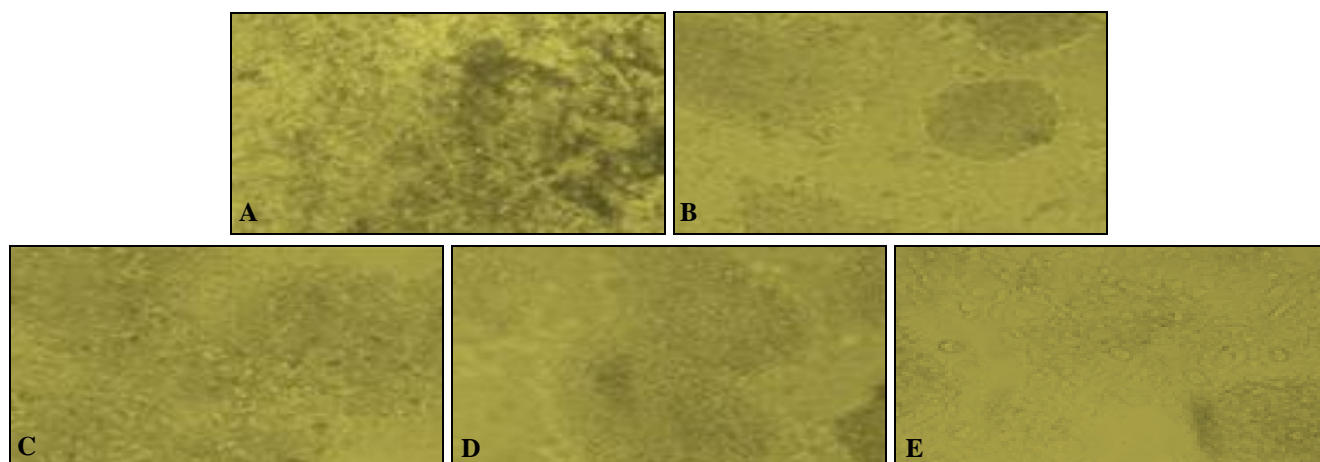


FIG. 9: MORPHOLOGICAL ANALYSIS OF NON-ENCAPSULATED ASTAXANTHIN AGAINST HepG2 CELL LINE – MTT ASSAY

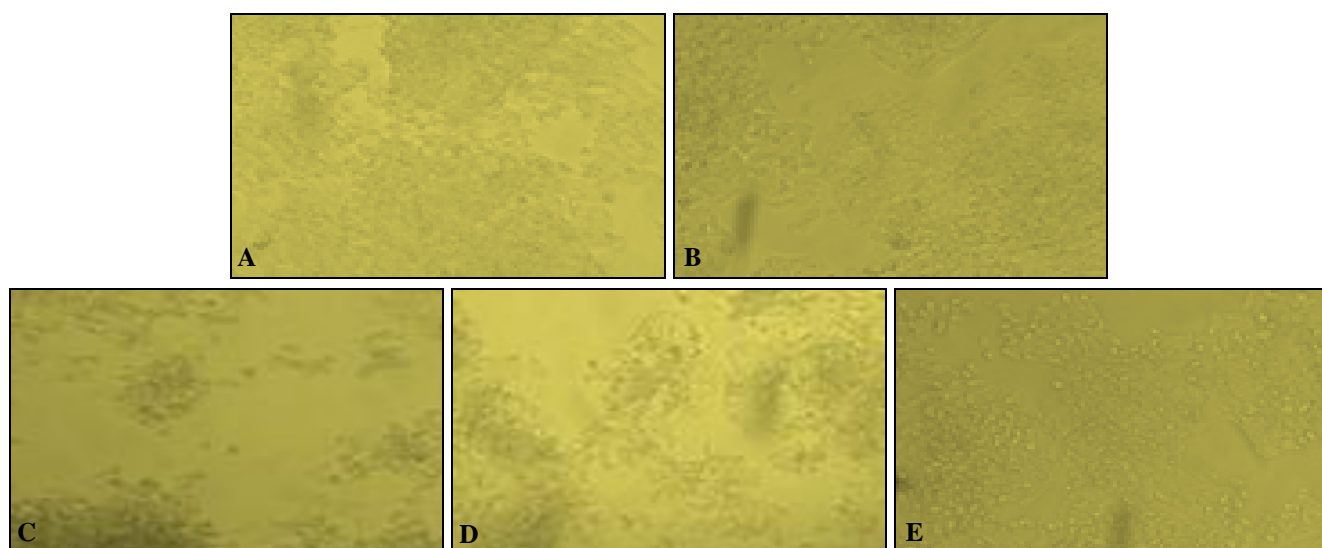


FIG. 10: MORPHOLOGICAL ANALYSIS OF ENCAPSULATED ASTAXANTHIN (ME1) AGAINST HepG2 CELL LINE – MTT ASSAY

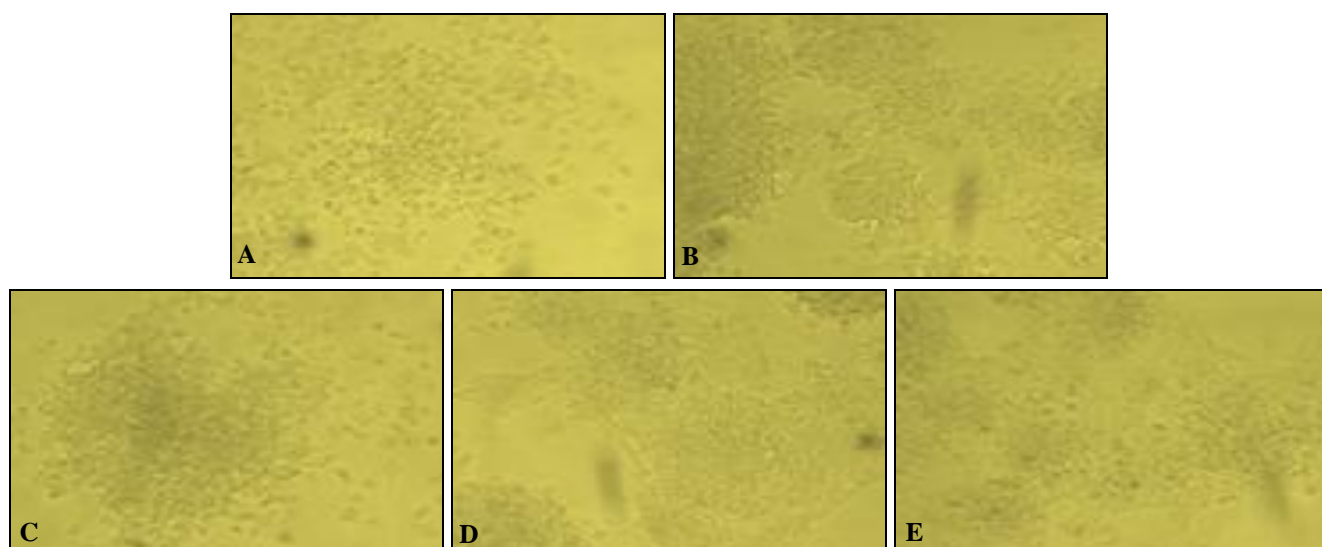


FIG. 11: MORPHOLOGICAL ANALYSIS OF ENCAPSULATED ASTAXANTHIN (ME2) AGAINST HepG2 CELL LINE – MTT ASSAY

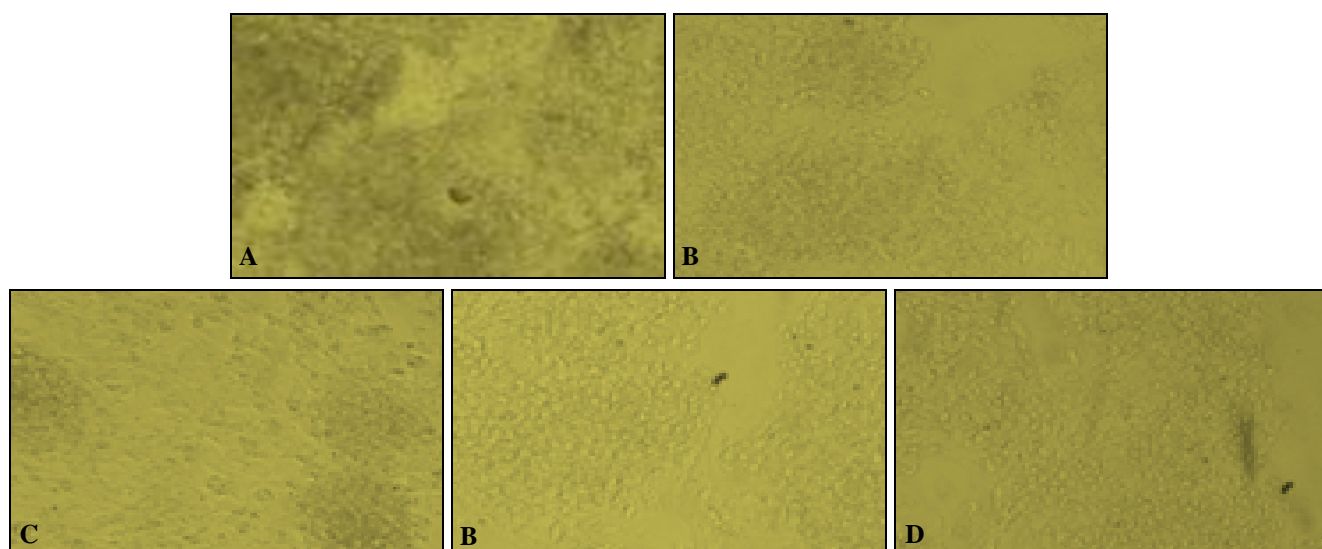


FIG. 12: MORPHOLOGICAL ANALYSIS OF ENCAPSULATED ASTAXANTHIN (ME3) AGAINST HepG2 CELL LINE – MTT ASSAY

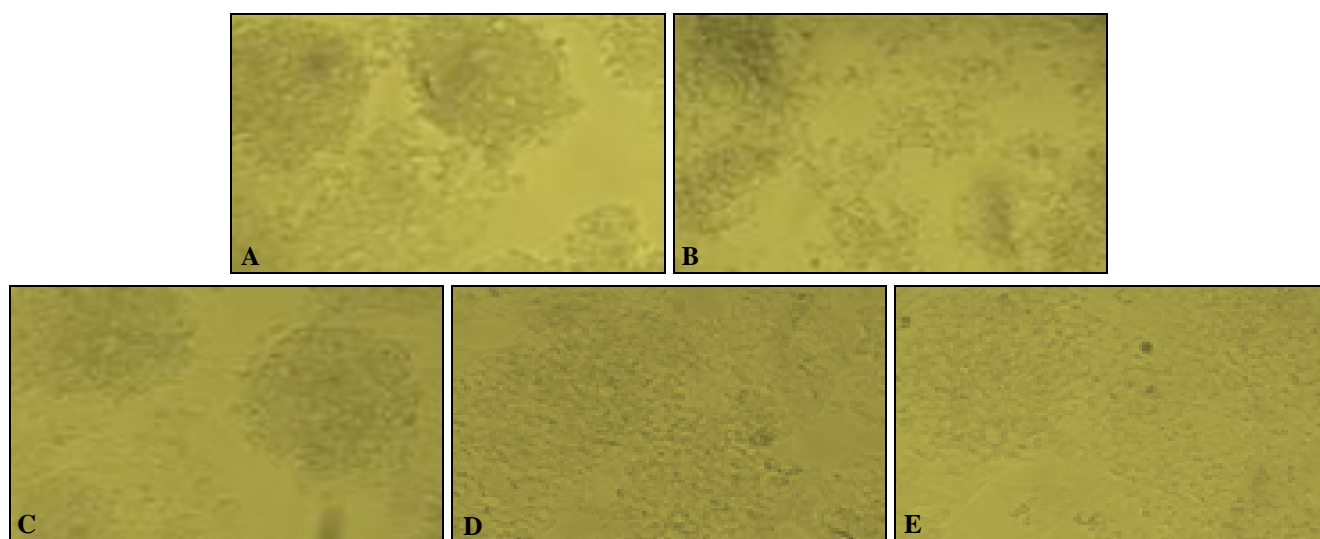


FIG. 13: MORPHOLOGICAL ANALYSIS OF ENCAPSULATED ASTAXANTHIN (ME4) AGAINST HepG2 CELL LINE – MTT ASSAY

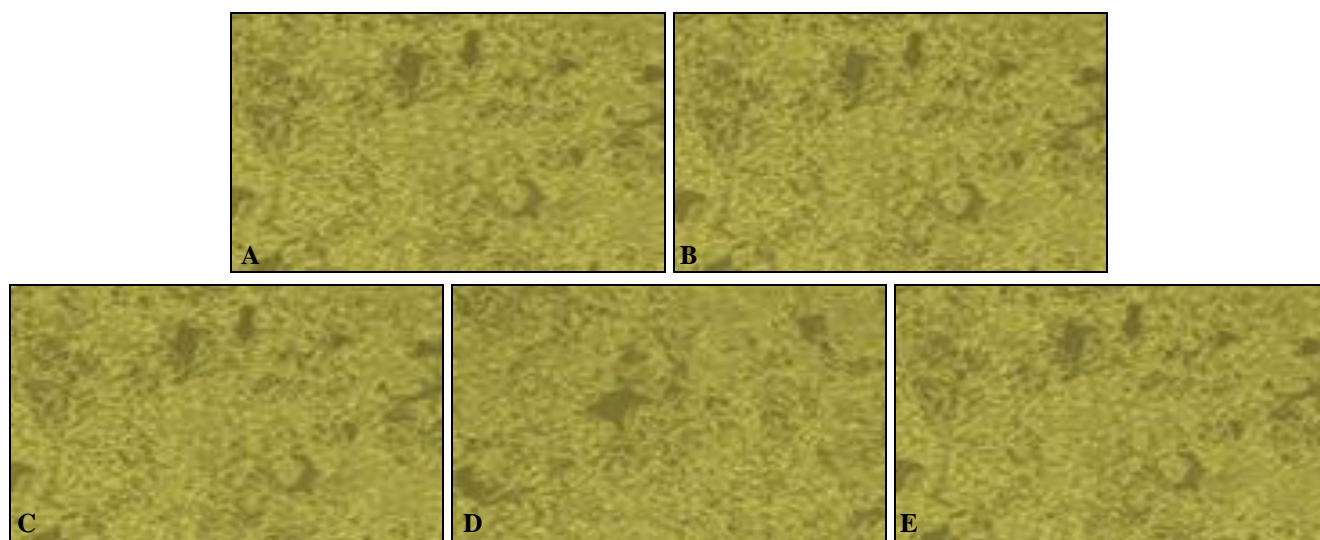


FIG. 14: MORPHOLOGICAL ANALYSIS OF POSITIVE DRUG SORAFENIB AGAINST HepG2 CELL LINE – MTT ASSAY

In this study, the antiproliferative effects of encapsulated astaxanthin (ME1, ME2, ME3 & ME4), non-encapsulated astaxanthin and sorafenib were tested on hepatocarcinoma cell line *i.e.* HepG2 assessed by MTT assay. At different concentrations: 200, 400, 600, 800 & 1000 $\mu\text{g/ml}$ dose-dependent inhibition was detected. The IC_{50} value for HepG2 was recorded as 500 $\mu\text{g/ml}$ after 24 h. A significant decrease in the cell viability was noted in treated groups when compared with the control one ($p < 0.05$). The result of the present study reveals that, the HepG2 cell line treated with liposomal encapsulated astaxanthin (ME4) along with positive drug sorafenib showed cell death up to 70% at concentration 800 $\mu\text{g/ml}$. the cells treated with the test drugs showed shrinkage which may be due to cell death induced by apoptosis **Fig. 8 -14**.

The cytotoxic activity induced by Non-encapsulated astaxanthin, ME1, ME2, ME3, ME4, and sorafenib involves apoptotic changes and nuclear condensation which was confirmed by the PI staining method. HepG2 cells showed a minor amount of PI-positive cells in the control group. In the group of cells treated at IC_{50} concentration of test drug along with positive drug for 24 h showed a tremendous increase in the number of Propidium iodide positive cells.

The overall results of this analysis projected that liposomal encapsulated astaxanthin (ME4) produces good activity when compared with the control, other group of drugs, and sorafenib. The diagrammatic representation was shown in **Fig. 15**.

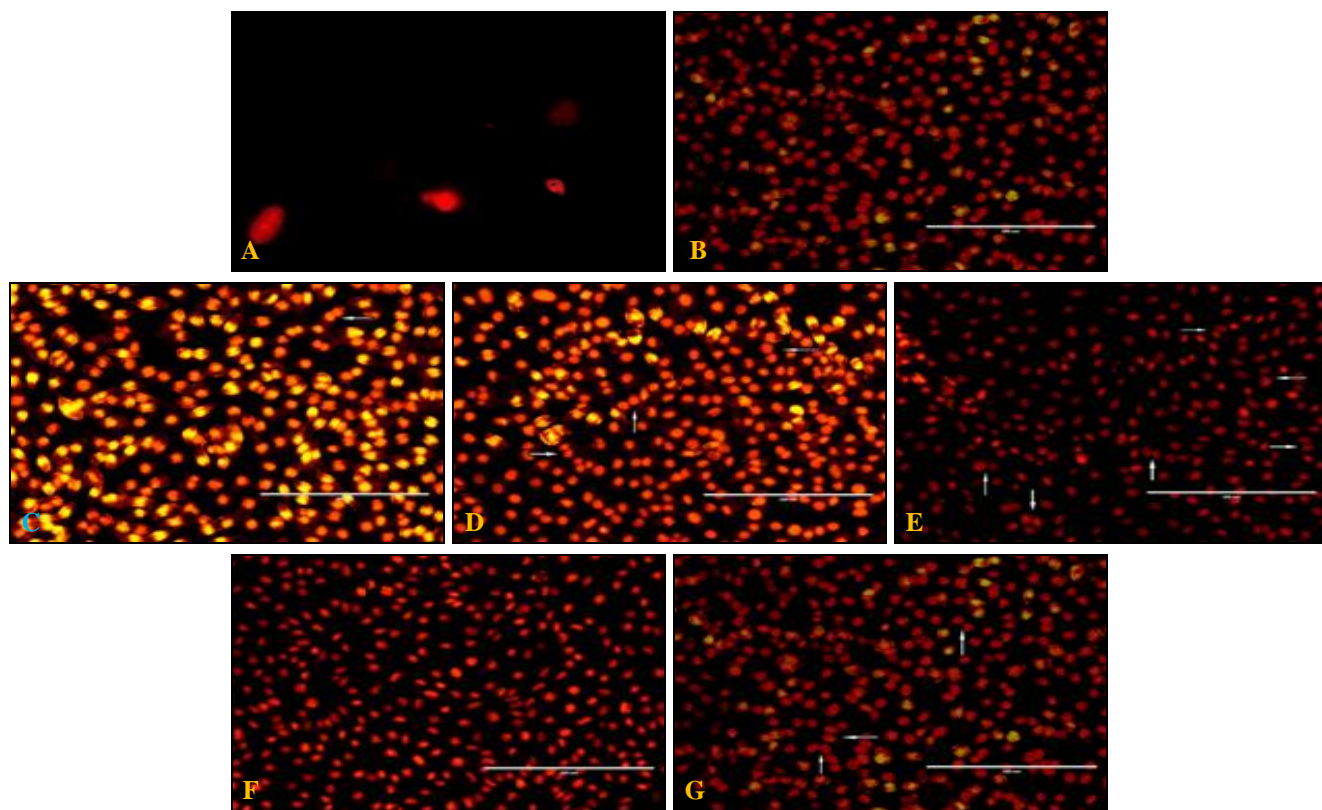


FIG. 15: EFFECT OF TEST DRUGS ON HepG2 CELLS AT 24 h STRAINED WITH PROPIDIUM IODIDE

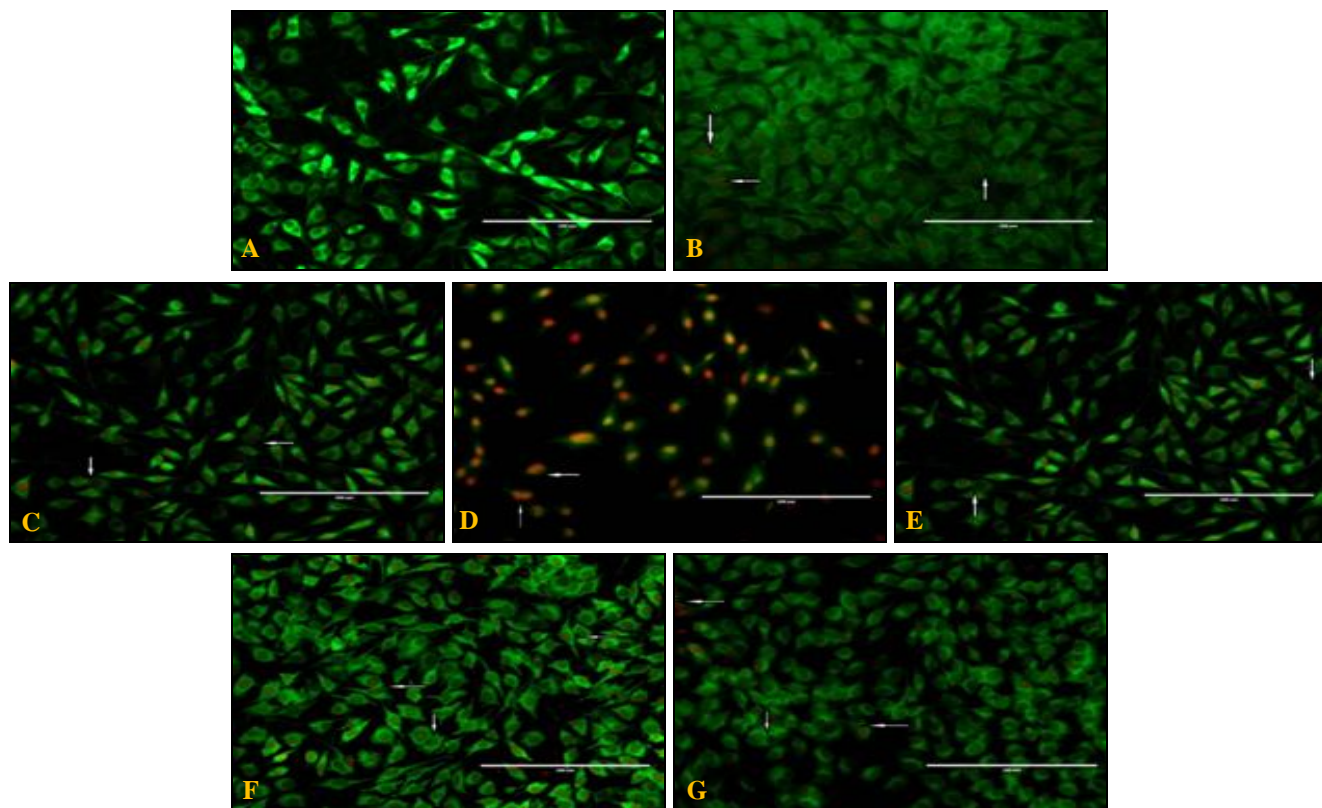


FIG. 16: EFFECT OF TEST DRUGS ON HepG2 CELLS AT 24 h STRAINED WITH ACRIDINE ORANGE AND ETHIDIUM BROMIDE. Note: A- Control; B- Non-encapsulated astaxanthin; C- ME1; D- ME2; E- ME3; F- ME4; G- Sorafenib

In the present study, HepG2 cells were treated with IC_{50} concentration of Non-encapsulated astaxanthin, ME1, ME2, ME3, ME4, and sorafenib,

which was allowed to stand for 24 h. After that, the cells were stained with AO/EB fluorescence staining that showed morphological apoptotic

changes when compared to untreated control cells. Arrow marks indicate the apoptotic cells. As shown in **Fig. 16**, HepG2 cells in the control group seemed to be in bright green with normal cell morphology, while the cells treated with IC_{50} concentration of all the test drugs for 24 h revealed an increased number of orange- and red-stained cells in a dose-dependent manner. Also, characteristic changes of apoptosis, including condensation and fragmentation of nucleus and formation of apoptotic bodies, were observed in the cells treated with different test drugs. From these results, we confirmed that liposomal encapsulated astaxanthin significantly induced apoptosis in HepG2 cells when compared to other test drugs and positive drug sorafenib.

In the present investigation, HepG2 cells were treated with IC_{50} concentration of Non-encapsulated astaxanthin, ME1, ME2, ME3, ME4, and sorafenib for 24 h that revealed decrement in the cell persistence by induction of DNA

fragmentation. **Fig. 17** represents the induction of apoptosis in scattering smears in the lanes by different test drugs (Non-encapsulated astaxanthin, ME1, ME2, ME3, ME4, and sorafenib). The smearing may be due to some post-apoptotic cell necrosis. When comparing the test drugs with the control, it is founded that the DNA present in the untreated control cells did not show any fragmentation or smearing.

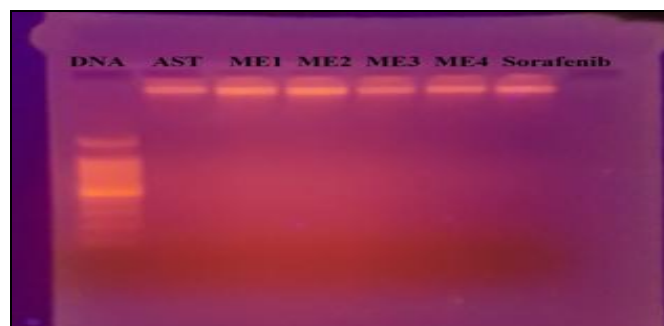


FIG. 17: DNA FRAGMENTATION OF HepG2 CELLS TREATED WITH TEST DRUGS

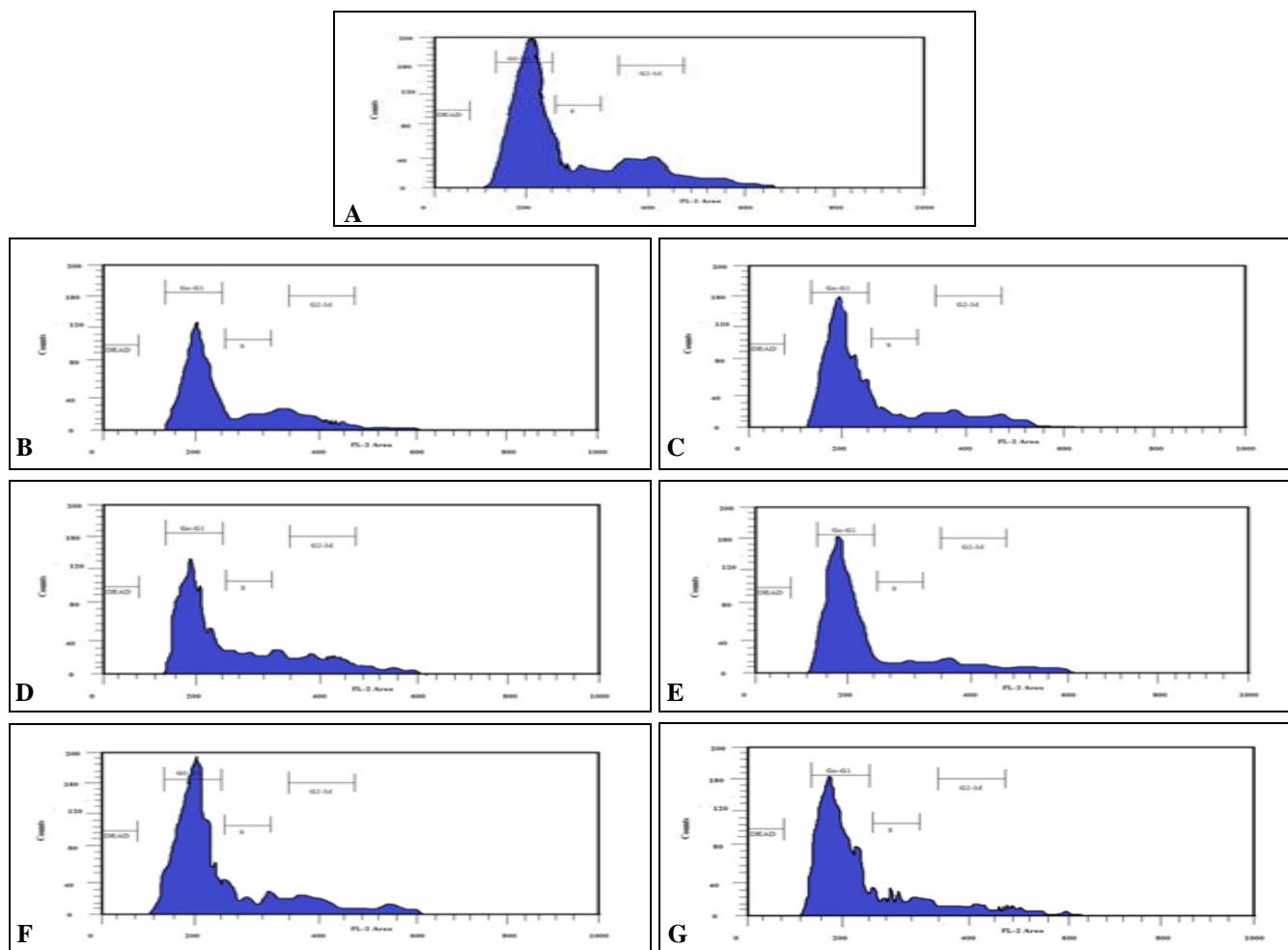


FIG. 18: FLOW CYTOMETRY ANALYSIS OF CELL CYCLE OF HepG2 CELL TREATED WITH IC_{50} CONCENTRATION OF TEST DRUGS

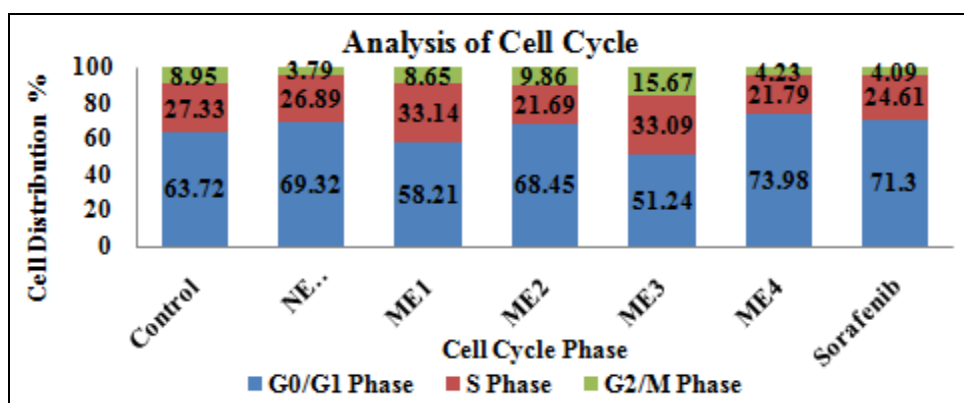


FIG. 19: FLOW CYTOMETRY ANALYSIS OF CELL CYCLE

In our present research work, HepG2 cells were treated with IC_{50} concentration of Non-encapsulated astaxanthin, ME1, ME2, ME3, ME4 and sorafenib for 24 h showed high percentage of apoptosis in sub G0-G1 phase ($69.32 \pm 0.12\%$, 58.21 ± 0.53 , $68.45 \pm 0.11\%$, $51.24 \pm 0.32\%$, $73.98 \pm 0.44\%$, $71.30 \pm 0.66\%$) when compared to control ($63.72 \pm 0.18\%$). The proportion of S phase was significantly increased in Non-encapsulated astaxanthin ($26.89 \pm 0.26\%$), ME1 ($33.14 \pm 0.46\%$), ME2 ($21.69 \pm 0.22\%$), ME3 ($33.09 \pm 0.09\%$), ME4 ($21.79 \pm 0.51\%$) and sorafenib ($24.61 \pm 0.71\%$) to that of control (27.33 ± 0.16) **Fig. 18**. There were no significant properties were noted in G0/G1 and G2/M phases. Thus, the result represents that the HepG2 cells treated with ME4 showed a high stimulation of apoptosis when compared to other test drugs and control group for 24 h in sub-G0-G1 phase.

DISCUSSION: Astaxanthin plays a main role in industrial, pharmaceutical, and biomedical uses. Encapsulated astaxanthin was not tested against cancer disease. Hence, we have first encapsulated the astaxanthin using different solvents, and there *in vitro* antioxidant, anti-inflammatory activities were determined, which has been reported in our previous articles^{26,27}.

The result shows good activity by encapsulated astaxanthin when compared to the free form of drug. The strategic factors in estimating the biocompatibility of encapsulated and non-encapsulated astaxanthin are cytotoxicity and cell viability. The cytotoxicity of the drugs under *in-vitro* conditions on Vero and HepG2 cells was examined in terms of encapsulated and non-encapsulated form on cell proliferation by MTT assay.

Tumor formation is categorized by the rapid proliferation of cancer cells. Cancer cells proliferate, stimulates their invasion, migrate, and adhere to target tissue. These steps allow the tumor cell to attain a metastatic phenotype. The signals transmitted by growth factors and adhesion proteins induce cell proliferation²⁸. The consequence of Astaxanthin on cell proliferation in cancer cells has been explored by many researchers. Induction of HepG2 cell apoptosis was characterized by the changes in cell morphology of the treated cells which were determined using AO/EB double staining. AO is a vital dye that stains both live and dead cells as it can penetrate the normal cell membrane. EB stains only cells that have lost their membrane integrity.

Cells that stained green indicate viable cells, yellow indicates early apoptosis, and orange/red indicates late apoptosis^{29, 30}. This technique combines the differential uptake of fluorescent DNA binding dyes of AO and EB and the morphologic feature of chromatin condensation in the stained nucleus, allowing one to discriminate among viable, apoptotic, and necrotic cells. The AO is used up by both viable and nonviable cells and emits either green fluorescence as a consequence of intercalation into double-stranded nucleic acids (generally DNA), or red fluorescence as a consequence of binding to single-stranded nucleic acids (generally RNA). The EB is utilized only by nonviable cells and emits red fluorescence by intercalation into DNA. Thus a viable cell retains a uniform bright green nucleus and orange cytoplasm. An initial apoptotic cell, whose membrane is still intact but then it has started to cleave its DNA, still has a green nucleus, but the chromatin of the cell turns out to be visible,

resulting from condensation in the form of bright green patches. A late apoptotic cell demonstrates bright orange areas of condensed chromatin in the nucleus (EB predominates over AO), and a necrotic cell indicates a uniform bright orange nucleus³¹.

The progression of programmed cell death (PCD) that occurs in multicellular organisms and comprises of many cellular events including nuclear fragmentation, cellular blebbing, chromosomal DNA fragmentation, and ultimately cell death is called apoptosis. In the physiological state, apoptosis is supported by a regulated process, conferring an advantage during an organism's life cycle occurs. Conversely, if apoptosis occurs in tumor cells, the tumor volume would decline, hence diminishing tumor burden and raising life expectancy.

In this regard, the effect of Astaxanthin on apoptosis has been studied by many researchers. The results achieved by¹¹ revealed that a significant peak of hypodiploid indicative of apoptosis was detected by flow cytometry when the cells were treated with astaxanthin. Besides, astaxanthin produced changes in mitochondria morphology, transmembrane potential, and respiratory chain and regulated apoptotic proteins in mitochondria, for example, B-cell lymphoma 2 (Bcl-2) and Bcl-2-associated X protein (Bax). In a hamster model of oral cancer,³² reported that Astaxanthin could induce caspase-mediated mitochondrial apoptosis by down-regulating the expression of anti-apoptotic Bcl-2. In another study, Astaxanthin decreased the expression of Bcl-2, B-cell lymphoma-extra-large (Bcl-xL), and c-myc while increased the level of Bax and non-metastasis23-1 (nm23-1) in a hepatocellular carcinoma cell line¹².

The inhibition of the cell cycle has to turn out to be an appreciated target for the management and usage of tumor cells with cytotoxic agents. Numerous anti-cancer agents and DNA-damaging agents capture the cell cycle at the G0/G1, S, or G2/M phase and then prompt apoptotic cell death. The cell cycle comprises four distinctive phases (G1 phase, S phase, G2 phase, and Mitosis) and two checkpoints (G0/G1 and G2/M checkpoints), which assure that no DNA damage is transferred to daughter cells³³.

CONCLUSION: The overall result of the present study shows that astaxanthin encapsulated by liposomal method provides good *in-vitro* anticancer activity in HepG2 Cell lines and also non-toxic to the Vero (Normal) Liver cell lines when compared to other methods of encapsulation and free form of the drug. However, the extract has to be tested on the animal by the *in-vivo* model to confirm their exact mechanism. Thus, the encapsulated astaxanthin has potential in the treatment and prevention of Hepatocellular carcinoma (HCC).

ACKNOWLEDGEMENT: The authors thank Mohamed Sathak College of Arts & Science for the use of research facilities.

CONFLICTS OF INTEREST: The authors declare no conflict of interest.

REFERENCES:

1. Tyagi N, Sharma GN, Shrivastava B, Saxena O and Kumar N: Medicinal plants: used in anticancer treatment. International Journal of Research and Development in Pharmacy and Life Science 2017; 6(5): 2732-39.
2. Berasain C: Hepatocellular carcinoma and sorafenib: too many resistance mechanisms. Gut 2013; 62: 1674-85.
3. Forner A, Llovet JM and Bruix J: Hepatocellular carcinoma. Lancet 2012, 379:1245-55.
4. Mesallamy HO, Metwally NS, Soliman MS, Ahmed KA and El Mesallamy MM: The chemopreventive effect of *Ginkgo biloba* and *Silybum marianum* extracts on hepatocarcinogenesis in rats. Cancer Cell International 2011; 11: 1-12.
5. Liu L, Cao Y, Chen C, Zhang X, McNabola A, Wilkie D, Wilhelm S, Lynch M and Carter C: Sorafenib blocks the RAF/MEK/ERK pathway, inhibits tumor angiogenesis, and induces tumor cell apoptosis in hepatocellular carcinoma model PLC/PRF/5. Cancer Res 2006, 66: 11851-58.
6. Cheng AL, Kang YK, Chen Z, Tsao CJ, Qin S, Kim JS, Luo R, Feng J, Ye S, Yang TS, Xu J, Sun Y, Liang H, Liu J, Wang J, Tak WY, Pan H, Burock K, Zou J, Voliotis D and Guan Z: Efficacy and safety of sorafenib in patients in the Asia-Pacific region with advanced hepatocellular carcinoma: a phase III randomised, double-blind, placebo-controlled trial. Lancet Oncology 2009; 10: 25-34.
7. Llovet JM, Ricci S, Mazzaferro V, Hilgard P, Gane E, Blanc JF, de Oliveira AC, Santoro A, Raoul JL, Forner A, Schwartz M and Porta C: Sorafenib in advanced hepatocellular carcinoma. The New England Journal of Medicine 2008, 359: 378-90.
8. Ambati RR, Phang SM, Ravi S and Aswathanarayana RG: Astaxanthin: Sources, extraction, stability, biological activities and its commercial applications-A review. Marine Drugs 2014; 12: 128-52.
9. Jiao G, Hui JPM, Burton IW, Thibault MH, Pelletier C, Boudreau J, Tchoukanova N, Subramanian B, Djaoued Y, Ewart S, Gagnon J, Ewart KV and Zhang J: Characterization of shrimp oil from *Pandalus borealis* by high performance liquid chromatography and high

- resolution mass spectrometry. *Marine Drugs* 2015; 13: 3849-76.
10. Megdal PA, Craft NA and Handelman GJ: A simplified method to distinguish farmed (*Salmo salar*) from wild salmon: Fatty acid ratios versus astaxanthin chiral isomers. *Lipids* 2009; 44: 569-76.
 11. Song XD, Zhang JJ, Wang MR, Liu WB, Gu XB and Lv CJ: Astaxanthin induces mitochondria-mediated apoptosis in rat hepatocellular carcinoma CBRH-7919 cells. *Biological and Pharmaceutical Bulletin* 2011; 34: 839-44.
 12. Song X, Wang M, Zhang L, Zhang J, Wang X, Liu W, Gu X and Lv C: Changes in cell ultrastructure and inhibition of JAK1/STAT3 signaling pathway in CBRH-7919 cells with astaxanthin. *Toxicology Mechanism and Methods* 2012; 22: 679-86.
 13. Suganya V, Anuradha V, Syed Ali M, Sangeetha P and Bhuvana P. Microencapsulation and characterization of astaxanthin prepared using different agents. *Research Journal of Chemical Sciences* 2017a; 7: 1-10.
 14. Lin SF, Chen YC, Chen RN, Chen LC, Ho HO, Tsung YH, Sheu MT and Liu DZ: Improving the Stability of Astaxanthin by Microencapsulation in Calcium Alginate Beads. *PLoS One* 2016; 11(4): 1-10.
 15. Park SA, Ahn JB, Choi SH, Lee JS and Lee HG: The effects of particle size on the physicochemical properties of optimized astaxanthin-rich *Xanthophyllomyces dendrorhous*- loaded microparticles. *LWT-Food Science and Technology* 2014; 55: 638-44.
 16. Klinkenberg G, Lystad K, Levine D and Dyrset N: pH-controlled cell release and biomass distribution of alginate-immobilized *Lactococcus lactis* sp. *lactis*. *Journal of Applied Meteorology* 2001; 91: 705-14.
 17. Krasaekoopt W, Bhandari B and Deeth H: Survival of probiotics encapsulated in chitosan-coated alginate beads in yoghurt from UHT- and conventionally treated milk during storage. *Food Sci and Technol* 2006; 39: 177-83.
 18. Krasaekoopt W, Bhandari B and Deeth H: The influence of coating materials on some properties of alginate beads and survivability of microencapsulated probiotic bacteria. *International Dairy Journal* 2004; 14: 737-43.
 19. Thamaket P and Raviyan P: Preparation and physical properties of carotenoids encapsulated in chitosan cross linked triphosphate nanoparticles. *Food and Applied Bioscience Journal* 2015; 3 (1): 69-84.
 20. Yangchao L, Boce Z, Monica W, Liangli Y and Qin W: Preparation and characterization of zein/chitosan complex for encapsulation of alpha tocopherol and its *In-vitro* controlled release study. *Colloids and Surfaces B: Biointerfaces* 2011; 85: 145-52.
 21. Chiu CH, Chang CC, Lin ST, Chyau CC and Peng RY: Improved Hepatoprotectivity effect of Liposome-encapsulated astaxanthin in lipopolysaccharide-induced acute hepatotoxicity. *International Journal of Molecular Sciences* 2016; 17: 1-17.
 22. Mossmann T: Rapid colorimetric assay for cellular growth and survival: application to proliferation and cytotoxicity assays. *J of Immunological Methods* 1983; 65: 55-63.
 23. Jeyaraj M, Rajesh M, Arun R, Ali M, Sathishkumar G, Sivanandhan G, Kapildev G, Manickavasagam M, Premkumar K, Thajuddin N and Ganapathi A: An investigation on the cytotoxicity and caspase-mediated apoptotic effect of biologically synthesized silver nanoparticles using *Podophyllum hexandrum* on human cervical carcinoma cells. *Colloids Surf. B: Biointerfaces* 2013; 102; 708-17.
 24. Bortner CD, Oldenburg NBE and Cidlowski JA: The role of DNA fragmentation in apoptosis. *Trends Cell Biology* 1995; 5 (1): 21-26.
 25. Pozarowski P and Darzynkiewicz Z: Analysis of cell cycle by flow cytometry. *Methods in Molecular Biology* 2004; 281: 301-11.
 26. Suganya V, Anuradha V, Ali MS, Sangeetha P and Bhuvana P: *In-vitro* antioxidant activity of micro-encapsulated and non-encapsulated astaxanthin. *Asian Journal of Science and Technology* 2017a; 8 (11): 6391-6404.
 27. Suganya V, Anuradha V, Ali MS, Sangeetha P and Bhuvana P: *In-vitro* anti-inflammatory activity of micro-encapsulated and non-encapsulated astaxanthin. *International Journal of Chem Tech Research* 2017b; 10(10): 186-95.
 28. Zhang L and Wang H: Multiple mechanisms of anticancer effects exerted by astaxanthin. *Marine Drugs* 2015; 13: 4310-30.
 29. Vijayan P, Viswanathamurthi P, Silambarasan V, Velmurugan D, Velmurugan K, Nandhakumar R, Butcher RJ, Silambarasan T and Dhandapani R: Dissymmetric thiosemicarbazone ligands containing substituted aldehyde arm and their ruthenium(II) carbonyl complexes with PPh₃/AsPh₃ as ancillary ligands: Synthesis, structural characterization, DNA/BSA interaction and *In vitro* anticancer activity. *J. Organometallic Chemistry* 2014; 768: 163-77.
 30. Mohankumar K, Pajaniradje S, Sridharan S, Singh VK, Ronsard L, Banerjee AC, Benson CS, Coumar MS and Rajagopalan R: Mechanism of apoptotic induction in human breast cancer cell, MCF-7, by an analog of curcumin in comparison with curcumin-An *in-vitro* and *in-silico* approach. *Chemico Biological Interaction* 2014; 210: 51-63.
 31. Atale N, Gupta S, Yadav UCS and Rani V: Cell-death assessment by fluorescent and non-fluorescent cytosolic and nuclear staining techniques. *Journal of Microscopy* 2014; 255(1): 7-19.
 32. Kavitha K, Kowshik J, Kishore TK, Baba AB and Nagini S: Astaxanthin inhibits NF-kappaB and Wnt/beta-catenin signaling pathways *via* inactivation of Erk/MAPK and PI3K/Akt to induce intrinsic apoptosis in a hamster model of oral cancer. *Biochimica Biophysica Acta* 2013; 1830: 4433-44.
 33. Shih SC and Stutman O: Cell cycle-dependent tumor necrosis factor apoptosis, *Cancer Research* 1996; 56: 1591-98.

How to cite this article:

Suganya V and Anuradha V: Cytoprotective role of encapsulated astaxanthin against hepatocellular carcinoma (HepG2) cell line. *Int J Pharm Sci & Res* 2021; 12(1): 372-84. doi: 10.13040/IJPSR.0975-8232.12(1).372-84.

All © 2013 are reserved by the International Journal of Pharmaceutical Sciences and Research. This Journal licensed under a Creative Commons Attribution-NonCommercial-ShareAlike 3.0 Unported License.

This article can be downloaded to **Android OS** based mobile. Scan QR Code using Code/Bar Scanner from your mobile. (Scanners are available on Google Playstore)